The Crystal Structures of $(+)_{589}$- and $(-)_{589}$-*trans*(*O*)-Ethylenediaminebis(glycinato)cobalt(III) Hydrogen-*d*-tartrates and Their Thermal Behavior

Masahiro KURAMOTO

Department of Chemistry, Faculty of Science, Hiroshima University, Higashi-senda-machi, Hiroshima 730

(Received October 27, 1978)

The crystal structures of two diastereoisomeric salts, $(+)_{589}$-*trans*(*O*)-[Co(gly)$_2$en]H-*d*-tart·3H$_2$O (**1**) and $(-)_{589}$-*trans*(*O*)-[Co(gly)$_2$en]H-*d*-tart·H$_2$O (**2**), have been determined by three-dimensional X-ray analysis. The less-soluble salt (**1**) is monoclinic; space group, $P2_1$; $Z=2$, $a=12.351(5)$, $b=7.671(3)$, $c=10.189(5)$ Å, and $\beta=110.71(4)°$ ($R=0.043$, 2241 reflections). The more-soluble salt (**2**) is monoclinic; space group, $P2_1$; $Z=2$, $a=11.135(4)$, $b=10.037(3)$, $c=7.716(3)$ Å, and $\beta=98.61(3)°$ ($R=0.064$, 2076 reflections). A comparison of the (unit cell volume)/Z values of the two crystals shows that the crystal **1** is more tightly packed than the crystal **2**. In both salts, adjacent complex cations form quite similar chain structures linked by (N–H···O) hydrogen bonds. The H-*d*-tart anions in **1** take a characteristic "head-to-tail" arrangement of an infinite chain of $\{$H-*d*-tart$\}_\infty$ along the b-axis. In contrast, this arrangement is not found in the more-soluble salt (**2**). From these findings, it can be considered that the discrimination of optical isomers in the H-*d*-tart system originates from the spiral chain structure of $\{$H-*d*-tart$\}_\infty$. The absolute configurations of $(+)_{589}$- and $(-)_{589}$-*trans*(*O*)-[Co(gly)$_2$en]$^+$ are determined to be Λ-δ and Δ-λ respectively. TG and DSC measurements were carried out for both salts, and the ΔH values of the dehydration step were estimated to be 64.4 kJ mol^{-1} for **1** and 73.0 kJ mol^{-1} for **2**.

Optical resolutions of metal complex ions are performed mostly through fractional crystallization utilizing the difference in solubilities of diastereoisomeric salts. However, no general rule has yet been established to judge what sort of a resolving agent is most effective for a particular racemic complex. To approach this problem, the X-ray crystal analysis of a pair of diastereoisomeric salts is indispensable. A comparison of the crystal structures of the less- and more-soluble diastereoisomeric salt pair will give an important clue for elucidating the mechanism of optical resolution.

With this expectation, the crystal structures were investigated recently for a pair of a less-soluble salt, $(+)_{589}$-[Co(ox)en$_2$]H-*d*-tart·H$_2$O (**3**), and a more-soluble salt, $(-)_{589}$-[Co(ox)en$_2$]H-*d*-tart·2H$_2$O (**4**);[1,2] their thermal behavior was also examined. It was found that, in **3**, complex cations are locked tightly in a space formed by four spiral chains of H-*d*-tart(*d*-$C_4H_5O_6^-$, abbr. H-*d*-tart) anions related by a twofold screw axis, while in **4**, complex cations are packed loosely in the four chains of the H-*d*-tart anion formed by a translation operation.[2]

In the present study the crystal structures were determined for another pair of diastereoisomeric salts, $(+)_{589}$-*trans*(*O*)-[Co(gly)$_2$en]H-*d*-tart·3H$_2$O (**1**) and $(-)_{589}$-*trans*(*O*)-[Co(gly)$_2$en]H-*d*-tart·H$_2$O (**2**). The complex, *trans*(*O*)-[Co(gly)$_2$en]$^+$, is actually resolved by way of these diastereoisomeric salts, both of which have been reported to be obtained easily as single crystals.[3] In addition, since *trans*(*O*)-[Co(gly)$_2$en]$^+$ and [Co(ox)en$_2$]$^+$ have the same chemical formula, $C_6H_{16}N_4O_4Co$, the volumes of both cations can be expected to be nearly equal. Thus, the present diastereoisomeric pair is considered to be one of the most suitable examples for clarifying the nature of discrimination by the H-*d*-tart anion.

Contrary to the diastereoisomeric salts, [Co(ox)en$_2$]-H-*d*-tart·*n*H$_2$O, the number of the water of crystallization of *trans*(*O*)-[Co(gly)$_2$en]H-*d*-tart·*n*H$_2$O is larger in the less-soluble salt than that in the more-soluble one. To see the role of the water of crystallization in their crystal packing, the thermal behavior of both crystals was investigated by means of TG and DSC measurements.

Experimental

Preparation of Compound. (a) The Less-soluble Salt, $(+)_{589}$-trans(O)-[Co(gly)$_2$en]H-d-tart·3H$_2$O (1): The less-soluble salt (**1**) was prepared by the method of Dabrowiak and Cooke.[3]

Table 1. Crystal parameters of two diastereoisomeric pairs

Diastereoisomers	a/Å	b/Å	c/Å	β/°	Space group	D_m/g cm^{-3}	Z	D_c/g cm^{-3}	V/Å^3	V/Z/Å^3
$(+)_{589}$-*trans*(*O*)-[Co(gly)$_2$en] H-*d*-tart·3H$_2$O (**1**)	12.351(5)	7.671(3)	10.189(5)	110.71(4)	$P2_1$	1.72	2	1.73(1)	903.0(7)	451.5(4)
$(-)_{589}$-*trans*(*O*)-[Co(gly)$_2$en] H-*d*-tart·H$_2$O (**2**)	11.135(4)	10.037(3)	7.716(3)	98.61(3)	$P2_1$	1.67	2	1.69(1)	852.7(5)	426.4(3)
$(+)_{589}$-[Co(ox)en$_2$] H-*d*-tart·H$_2$O (**3**)[a]	8.256(3)	14.588(4)	7.009(1)	104.73(2)	$P2_1$	1.74	2	1.77(1)	816.4(4)	408.2(2)
$(-)_{589}$-[Co(ox)en$_2$] H-*d*-tart·2H$_2$O (**4**)[a]	16.583(5)	14.186(5)	7.403(2)	——	$P2_12_12$	1.72	4	1.73(1)	1741.5(10)	435.4(3)

1, **3**: The less-soluble salt. **2**, **4**: The more-soluble salt. a) The crystal data of **3** and **4** were remeasured in a manner similar to that used for **1** and **2**.

The crystals are hexagonal rods. Found: C, 25.52; H, 5.84; N, 11.80%. Calcd for $C_{10}H_{27}N_4O_{13}Co$: C, 25.54; H, 5.79; N, 11.91%.

(b) The More-soluble Salt, (−)$_{589}$-trans(O)-[Co(gly)$_2$en]H-d-tart·H$_2$O (2): After the removal of the precipitated crystals of the $(+)_{589}$-salt,[3] the filtrate was cooled in a refrigerator. The crystals **2** were thus separated out as rhombic plates. Found: C, 27.79; H, 5.40; N, 12.90%. Calcd for $C_{10}H_{23}N_4O_{11}Co$: C, 27.66; H, 5.33; N, 12.90%.

X-Ray Data Collection. Weissenberg photographs indicated a monoclinic unit cell with the systematic absence of $(0k0)$ when $k=2n+1$ for both **1** and **2**. Of the two possible space groups, $P2_1$ and $P2_1/m$, the latter was eliminated because of the optical activity of these compounds. The crystal sizes used for the cell constant and intensity measurements were $0.25\times0.50\times0.40$ mm^3 for **1** and $0.15\times0.20\times0.30$ mm^3 for **2**. All the cell constants were determined by a least-squares treatment of the setting of 15 reflections measured on a Syntex R3 computer-controlled four-circle diffractometer with Mo $K\alpha$ radiation ($\lambda=0.7107$ Å) monochromated by a graphite plate. All the cell constants are summarized in Table 1. The intensity data for **1** and **2** were collected by the ω-2θ scan technique to a maximum 2θ value of 55° at a scan rate of 3°/min. The intensities of 2366 and 2234 independent reflections were collected for **1** and **2** respectively. Reflections for which the intensities were less than three times their standard deviations were regarded as "unobserved" and were not included in subsequent calculations. Thus, 2241 and 2076 independent reflections were used for the structure determination for **1** and **2** respectively. Their intensities were corrected for Lorentz and polarization factors, but no absorption corrections were made since the μ-values (10.7 cm^{-1} for **1** and 11.2 cm^{-1} for **2**) were low.

Thermogravimetric Analysis (TG). The TG data were obtained with a Rigaku Thermal Analyzer (Model 8005). A heating rate of 3 K/min and a static air atmosphere were employed, and 7.65—11.13 mg samples were used in each run.

Differential Scanning Calorimetry (DSC). A Rigaku Differential Scanning Calorimeter (Model-8055Cl) was used to record the DSC curves. In order to determine the ΔH values of the dissociation of the water of crystallization for both diastereoisomers, the instrument was calibrated using the ΔH values of the fusion of pure indium, tin, and lead metals as standards. The weights of the samples were 9.20—13.75 mg. A heating rate of 10 K/min was used in each run. The dry nitrogen gas (25 ml/min) was used as the furnace atmosphere.

Determination and Refinement of Crystal Structures

The Less-soluble Salt, (+)$_{589}$-trans(O)-[Co(gly)$_2$en]H-d-tart·3H$_2$O (1). A three-dimensional Patterson function revealed the position of the cobalt atom. The remaining nonhydrogen atoms were located by an application of the Fourier method. Several cycles of block-diagonal least-squares refinement using isotropic thermal parameters reduced the R value (defined as $\Sigma||F_o|-|F_c||/\Sigma|F_o|$) to 0.118. Further refinement using both positional and anisotropic thermal parameters for the nonhydrogen atoms reduced the R value to 0.061. A difference map at this stage revealed the positions of all hydrogen atoms. The final refinement including the contribution of these hydrogen atoms with the fixed positions and isotropic temperature

Table 2. Final atomic parameters with their e.s.d.'s for $(+)_{589}$-*trans*(*O*)-[Co(gly)$_2$en]H-*d*-tart·3H$_2$O

Atom	x	y	z
Co	0.95978(4)	0.75000(15)	0.73971(5)
O(G1)	1.0157(3)	0.9326(5)	0.6554(3)
O(G2)	1.1642(3)	1.1084(6)	0.6820(4)
O(G3)	0.9150(3)	0.5634(5)	0.8314(4)
O(G4)	0.9144(5)	0.2769(5)	0.8447(5)
O(T1)	0.4805(6)	1.1188(8)	0.3802(5)
O(T2)	0.4541(4)	1.1484(6)	0.1508(5)
O(T3)	0.4164(3)	0.7776(5)	0.3446(4)
O(T4)	0.6187(3)	0.7852(5)	0.2747(5)
O(T5)	0.5280(4)	0.4693(6)	0.1915(5)
O(T6)	0.3716(3)	0.5788(6)	0.0285(4)
O(W1)	0.8057(4)	0.8685(7)	1.0940(5)
O(W2)	0.2421(4)	0.6179(11)	0.6641(9)
O(W3)	0.3159(4)	0.9126(9)	0.5350(5)
N(G1)	1.1145(3)	0.7530(7)	0.8859(4)
N(G2)	1.0025(4)	0.5731(6)	0.6299(4)
N(E1)	0.8068(3)	0.7697(7)	0.5903(4)
N(E2)	0.8985(4)	0.9086(6)	0.8470(5)
C(G1)	1.1174(4)	0.9886(7)	0.7248(5)
C(G2)	1.1787(5)	0.9083(8)	0.8689(5)
C(G3)	0.9266(4)	0.4103(7)	0.7861(5)
C(G4)	0.9578(5)	0.4037(7)	0.6535(5)
C(E1)	0.7430(6)	0.9177(11)	0.6241(7)
C(E2)	0.7718(5)	0.9183(12)	0.7783(7)
C(T1)	0.4554(5)	1.0577(7)	0.2620(6)
C(T2)	0.4230(4)	0.8696(7)	0.2257(5)
C(T3)	0.5073(4)	0.7794(6)	0.1673(5)
C(T4)	0.4643(4)	0.5934(7)	0.1239(5)
H(NG11)[a]	1.159	0.649	0.881
H(NG12)	1.107	0.761	0.981
H(NG21)	1.089	0.570	0.656
H(NG22)	0.968	0.606	0.526
H(NE11)	0.762	0.663	0.582
H(NE12)	0.817	0.796	0.498
H(NE21)	0.933	1.030	0.851
H(NE22)	0.918	0.868	0.946
H(CG21)	1.264	0.874	0.879
H(CG22)	1.185	1.002	0.948
H(CG41)	1.021	0.310	0.665
H(CG42)	0.884	0.374	0.567
H(CE11)	0.654	0.904	0.572
H(CE12)	0.769	1.038	0.592
H(CE21)	0.732	0.814	0.809
H(CE22)	0.740	1.037	0.809
H(CT2)	0.340	0.870	0.145
H(CT3)	0.512	0.846	0.077
H(OW11)	0.810	0.833	1.160
H(OW12)	0.726	0.867	1.052
H(OW21)	0.300	0.570	0.725
H(OW22)	0.282	0.700	0.640
H(OW31)	0.380	0.933	0.595
H(OW32)	0.352	0.880	0.485
H(OT2)	0.472	1.250	0.165
H(OT3)	0.488	0.763	0.412
H(OT4)	0.670	0.833	0.287

a) The averaged e.s.d.'s of hydrogen atoms are; $\overline{\sigma(x)}=0.008$, $\overline{\sigma(y)}=0.017$, and $\overline{\sigma(z)}=0.013$.

TABLE 3. ANISOTROPIC TEMPERATURE FACTORS ($\times 10^3$ Å^2) EXPRESSED IN THE FORM $\exp[-2\pi^2(U_{11}h^2a^{*2}+U_{22}k^2b^{*2}+U_{33}l^2c^{*2}+2U_{12}hka^*b^*+2U_{13}hla^*c^*+2U_{23}klb^*c^*)]$ FOR $(+)_{589}$-*trans*(*O*)-[Co(gly)$_2$en]H-*d*-tart·3H$_2$O

Atom	U_{11}	U_{22}	U_{33}	U_{12}	U_{13}	U_{23}
Co	20.4(2)	10.8(2)	14.6(2)	−1.1(2)	7.3(0)	−1.0(2)
O(G1)	24(2)	21(2)	19(1)	0(1)	8(1)	5(1)
O(G2)	28(2)	19(2)	37(2)	−6(2)	14(1)	4(2)
O(G3)	30(2)	13(2)	25(2)	−4(1)	17(1)	−3(1)
O(G4)	77(3)	12(2)	37(2)	−3(2)	31(2)	2(2)
O(T1)	104(4)	34(3)	36(2)	−13(3)	22(3)	−14(2)
O(T2)	57(3)	19(2)	40(2)	−5(2)	23(2)	−1(2)
O(T3)	40(2)	23(2)	27(2)	1(2)	17(1)	6(2)
O(T4)	20(2)	21(2)	50(2)	3(1)	4(2)	−8(2)
O(T5)	42(2)	18(2)	39(2)	−1(2)	7(2)	5(2)
O(T6)	32(2)	27(2)	31(2)	−6(2)	3(2)	−5(2)
O(W1)	37(2)	39(3)	39(2)	6(2)	11(2)	15(2)
O(W2)	33(2)	79(5)	104(5)	15(3)	31(3)	38(4)
O(W3)	32(2)	60(3)	46(2)	9(2)	11(2)	−11(3)
N(G1)	27(2)	16(2)	21(2)	2(2)	8(1)	4(2)
N(G2)	32(2)	16(2)	24(2)	−3(2)	17(2)	−4(2)
N(E1)	24(2)	23(2)	16(1)	−5(2)	4(1)	−1(2)
N(E2)	28(2)	11(2)	30(2)	−2(2)	16(2)	−6(2)
C(G1)	23(2)	15(2)	14(2)	5(2)	6(2)	5(2)
C(G2)	31(2)	29(3)	10(2)	−9(2)	−8(2)	8(2)
C(G3)	33(2)	9(2)	29(2)	−2(2)	12(2)	−4(2)
C(G4)	37(2)	10(2)	17(2)	−3(2)	9(2)	−4(2)
C(E1)	35(3)	52(4)	38(3)	14(3)	1(2)	−9(3)
C(E2)	29(3)	52(4)	44(3)	7(3)	8(2)	−14(3)
C(T1)	34(3)	13(3)	27(2)	2(2)	7(2)	−2(2)
C(T2)	24(2)	15(2)	22(2)	−3(2)	8(2)	0(2)
C(T3)	22(2)	10(2)	30(2)	−3(2)	9(2)	−5(2)
C(T4)	26(2)	16(2)	29(2)	−4(2)	11(2)	−2(2)

TABLE 4. FINAL ATOMIC PARAMETERS WITH THEIR e.s.d's FOR $(-)_{589}$-*trans*(*O*)-[Co(gly)$_2$en]H-*d*-tart·H$_2$O

Atom	x	y	z	Atom	x	y	z
Co	0.85377(8)	0.75000(20)	0.69785(10)	C(T4)	0.2135(8)	0.6848(8)	0.1366(10)
O(G1)	0.9259(5)	0.8542(6)	0.5361(8)	H(NG11)[a]	0.972	0.543	0.692
O(G2)	1.0975(6)	0.8810(7)	0.4260(9)	H(NG12)	1.046	0.647	0.830
O(G3)	0.7926(5)	0.6438(6)	0.8687(7)	H(NG21)	0.913	0.959	0.864
O(G4)	0.7904(8)	0.6223(7)	1.1514(8)	H(NG22)	1.018	0.847	0.918
O(T1)	0.4776(7)	0.9791(8)	0.1414(9)	H(NE11)	0.734	0.962	0.661
O(T2)	0.5172(10)	0.9229(11)	−0.1222(13)	H(NE12)	0.659	0.852	0.756
O(T3)	0.3919(6)	0.6892(7)	−0.1213(8)	H(NE21)	0.773	0.542	0.551
O(T4)	0.1960(5)	0.8569(6)	−0.0894(8)	H(NE22)	0.800	0.650	0.403
O(T5)	0.1116(6)	0.6420(7)	0.0641(9)	H(CG21)	1.059	0.610	0.475
O(T6)	0.2719(6)	0.6367(7)	0.2764(8)	H(CG22)	1.163	0.680	0.634
OW	0.3480(7)	0.7995(9)	0.5518(9)	H(CG41)	0.804	0.898	1.066
N(G1)	0.9973(6)	0.6361(7)	0.7105(9)	H(CG42)	0.938	0.829	1.162
N(G2)	0.9271(6)	0.8602(7)	0.8937(8)	H(CE11)	0.681	0.868	0.387
N(E1)	0.7090(6)	0.8637(8)	0.6614(10)	H(CE12)	0.550	0.871	0.477
N(E2)	0.7656(6)	0.6359(7)	0.5155(8)	H(CE21)	0.590	0.642	0.363
C(G1)	1.0314(7)	0.8157(7)	0.5095(9)	H(CE22)	0.589	0.639	0.584
C(G2)	1.0701(8)	0.6770(8)	0.5782(12)	H(CT2)	0.440	0.723	0.137
C(G3)	0.8159(9)	0.6880(9)	1.0268(10)	H(CT3)	0.276	0.889	0.159
C(G4)	0.8709(10)	0.8252(9)	1.0485(10)	H(OW1)	0.330	0.753	0.467
C(E1)	0.6388(8)	0.8280(12)	0.4896(14)	H(OW2)	0.290	0.875	0.520
C(E2)	0.6345(8)	0.6748(12)	0.4854(12)	H(OT1)	0.525	1.050	0.085
C(T1)	0.4696(7)	0.8968(11)	0.0049(12)	H(OT3)	0.393	0.743	−0.213
C(T2)	0.3971(7)	0.7740(8)	0.0282(10)	H(OT4)	0.230	0.943	−0.093
C(T3)	0.2698(7)	0.8084(8)	0.0651(10)				

a) The averaged e.s.d.'s of hydrogen atoms are; $\overline{\sigma(x)}=0.008$, $\overline{\sigma(y)}=0.014$, and $\overline{\sigma(z)}=0.015$.

TABLE 5. ANISOTROPIC TEMPERATURE FACTORS ($\times 10^3$Å^2) EXPRESSED IN THE FORM $\exp[-2\pi^2(U_{11}h^2a^{*2}+U_{22}k^2b^{*2}+U_{33}l^2c^{*2}+2U_{12}hka^*b^*+2U_{13}hla^*c^*+2U_{23}klb^*c^*)]$ FOR $(-)_{589}$-*trans*(*O*)-[Co(gly)$_2$en]H-*d*-tart·H$_2$O

Atom	U_{11}	U_{22}	U_{33}	U_{12}	U_{13}	U_{23}
Co	24.0(3)	16.2(4)	16.4(3)	0.2(1)	5.2(3)	0.4(4)
O(G1)	33(3)	19(3)	31(3)	3(2)	10(2)	4(2)
O(G2)	35(3)	28(3)	49(4)	−1(3)	16(3)	6(3)
O(G3)	37(3)	23(3)	22(2)	−8(2)	8(2)	−3(2)
O(G4)	90(6)	28(3)	24(3)	−14(4)	21(3)	−2(3)
O(T1)	60(4)	42(4)	38(4)	−15(4)	18(3)	−4(3)
O(T2)	94(7)	74(7)	66(6)	−34(6)	54(5)	−19(5)
O(T3)	43(3)	32(3)	35(3)	16(3)	6(3)	−3(3)
O(T4)	29(3)	24(3)	31(3)	−3(2)	−2(2)	4(3)
O(T5)	37(3)	29(3)	42(3)	−8(3)	2(3)	5(3)
O(T6)	47(4)	30(3)	28(3)	0(3)	0(3)	6(3)
OW	41(4)	66(5)	39(3)	−9(4)	2(3)	3(4)
N(G1)	31(3)	20(3)	32(3)	2(3)	10(3)	2(3)
N(G2)	30(3)	21(3)	22(3)	2(3)	−2(2)	−1(3)
N(E1)	24(3)	24(3)	38(4)	4(3)	12(3)	1(3)
N(E2)	36(3)	20(3)	19(3)	−3(3)	5(2)	−3(3)
C(G1)	31(4)	16(3)	20(3)	−4(3)	6(3)	−2(3)
C(G2)	35(4)	18(4)	42(4)	1(3)	25(3)	−5(3)
C(G3)	56(5)	18(3)	24(4)	0(4)	14(3)	−2(3)
C(G4)	67(6)	24(4)	16(3)	−7(4)	18(3)	−6(3)
C(E1)	31(4)	46(6)	47(5)	5(4)	−9(4)	4(5)
C(E2)	33(4)	52(6)	36(4)	−5(4)	−6(3)	−12(4)
C(T1)	16(3)	46(5)	41(4)	4(3)	0(3)	5(4)
C(T2)	29(3)	27(5)	26(3)	3(3)	2(3)	1(3)
C(T3)	26(3)	21(4)	26(3)	0(3)	2(3)	9(3)
C(T4)	36(4)	19(4)	26(4)	0(3)	10(3)	8(3)

TABLE 6. BOND DISTANCES AND ANGLES (e.s.d.'s IN PARENTHESES) FOR $(+)_{589}$-*trans*(*O*)-[Co(gly)$_2$en]H-*d*-tart·3H$_2$O

Bond distances [l/Å]

Co–O(G1)	1.897(4)	N(G1)–C(G2)	1.475(8)	O(T1)–C(T1)	1.226(10)
Co–O(G3)	1.896(4)	N(G2)–C(G4)	1.465(7)	O(T2)–C(T1)	1.324(8)
Co–N(G1)	1.964(6)	N(E1)–C(E1)	1.490(10)	O(T3)–C(T2)	1.429(7)
Co–N(G2)	1.947(5)	N(E2)–C(E2)	1.473(10)	O(T4)–C(T3)	1.425(7)
Co–N(E1)	1.969(5)	C(G1)–C(G2)	1.523(8)	O(T5)–C(T4)	1.272(7)
Co–N(E2)	1.958(5)	C(G3)–C(G4)	1.531(8)	O(T6)–C(T4)	1.217(7)
O(G1)–C(G1)	1.278(6)	C(E1)–C(E2)	1.483(12)	C(T1)–C(T2)	1.508(8)
O(G2)–C(G1)	1.244(7)			C(T2)–C(T3)	1.536(8)
O(G3)–C(G3)	1.288(7)			C(T3)–C(T4)	1.532(8)
O(G4)–C(G3)	1.220(8)				

Bond Aangles[ϕ/°]

O(G1)–Co–N(G1)	85.5(2)	O(G1)–C(G1)–C(G2)	117.0(5)
O(G3)–Co–N(G2)	86.7(2)	N(G1)–C(G2)–C(G1)	109.6(5)
N(E1)–Co–N(E2)	86.0(2)	O(G3)–C(G3)–C(G4)	116.1(5)
Co–O(G1)–C(G1)	116.2(3)	N(G2)–C(G4)–C(G3)	110.0(5)
Co–O(G3)–C(G3)	115.0(4)	N(E1)–C(E1)–C(E3)	107.4(7)
Co–N(G1)–C(G2)	109.9(4)	N(E2)–C(E2)–C(E1)	108.7(7)
Co–N(G2)–C(G4)	109.3(3)	O(G1)–C(G1)–O(G2)	122.8(5)
Co–N(E1)–C(E1)	108.8(4)	O(G3)–C(G3)–O(G4)	122.7(5)
Co–N(E2)–C(E2)	108.8(4)	O(G2)–C(G1)–C(G2)	120.2(5)
		O(G4)–C(G3)–C(G4)	121.2(5)
O(T1)–C(T1)–O(T2)	124.2(6)	O(T5)–C(T4)–O(T6)	126.2(6)
O(T1)–C(T1)–C(T2)	124.0(6)	O(T2)–C(T1)–C(T2)	111.8(5)
O(T3)–C(T2)–C(T1)	110.8(5)	O(T3)–C(T2)–C(T3)	110.8(4)
O(T4)–C(T3)–C(T2)	106.9(4)	O(T4)–C(T3)–C(T4)	113.2(4)
O(T5)–C(T4)–C(T3)	117.1(5)	O(T6)–C(T4)–C(T3)	116.7(5)
C(T1)–C(T2)–C(T3)	111.6(5)	C(T2)–C(T3)–C(T4)	108.6(4)

TABLE 7. BOND DISTANCES AND ANGLES (e.s.d.'s IN PARENTHESES) FOR $(-)_{589}$-*trans*(*O*)-[Co(gly)$_2$en]H-*d*-tart·H_2O

Bond distances [*l*/Å]

Co–O(G1)	1.897(6)	N(G1)–C(G2)	1.455(11)	O(T1)–C(T1)	1.330(4)
Co–O(G3)	1.899(6)	N(G2)–C(G4)	1.472(13)	O(T2)–C(T1)	1.211(16)
Co–N(G1)	1.955(7)	N(E1)–C(E1)	1.479(14)	O(T3)–C(T2)	1.428(11)
Co–N(G2)	1.950(7)	N(E2)–C(E2)	1.496(14)	O(T4)–C(T3)	1.428(11)
Co–N(E1)	1.960(8)	C(G1)–C(G2)	1.528(12)	O(T5)–C(T4)	1.262(11)
Co–N(E2)	1.960(7)	C(G3)–C(G4)	1.506(15)	O(T6)–C(T4)	1.269(11)
O(G1)–C(G1)	1.281(10)	C(E1)–C(E2)	1.539(17)	C(T1)–C(T2)	1.499(13)
O(G2)–C(G1)	1.236(10)			C(T2)–C(T3)	1.527(12)
O(G3)–C(G3)	1.287(12)			C(T3)–C(T4)	1.530(12)
O(G4)–C(G3)	1.234(13)				

Bond angles [ϕ/°]

O(G1)–Co–N(G1)	86.1(3)	O(G1)–C(G1)–C(G2)	115.9(7)
O(G3)–Co–N(G2)	86.2(3)	N(G1)–C(G2)–C(G1)	110.0(7)
N(E1)–Co–N(E2)	85.7(3)	O(G3)–C(G3)–C(G4)	116.2(9)
Co–O(G1)–C(G1)	115.3(5)	N(G2)–C(G4)–C(G3)	110.1(8)
Co–O(G3)–C(G3)	114.9(6)	N(E1)–C(E1)–C(E2)	105.8(9)
Co–N(G1)–C(G2)	109.7(3)	N(E2)–C(E2)–C(E1)	103.4(9)
Co–N(G2)–C(G4)	108.3(6)	O(G1)–C(G1)–O(G2)	123.7(7)
Co–N(E1)–C(E1)	107.5(6)	O(G3)–C(G3)–O(G4)	121.1(9)
Co–N(E2)–C(E2)	109.4(6)	O(G2)–C(G1)–C(G2)	120.3(7)
		O(G4)–C(G3)–C(G4)	122.6(10)
O(T1)–C(T1)–O(T2)	121.4(11)	O(T5)–C(T4)–O(T6)	124.0(8)
O(T1)–C(T1)–C(T2)	112.9(9)	O(T2)–C(T1)–C(T2)	125.7(10)
O(T3)–C(T2)–C(T1)	110.5(7)	O(T3)–C(T2)–C(T3)	111.1(7)
O(T4)–C(T3)–C(T2)	110.9(7)	O(T4)–C(T3)–C(T4)	111.2(7)
O(T5)–C(T4)–C(T3)	120.4(8)	O(T6)–C(T4)–C(T3)	115.4(7)
C(T1)–C(T2)–C(T3)	111.6(7)	C(T2)–C(T3)–C(T4)	109.0(7)

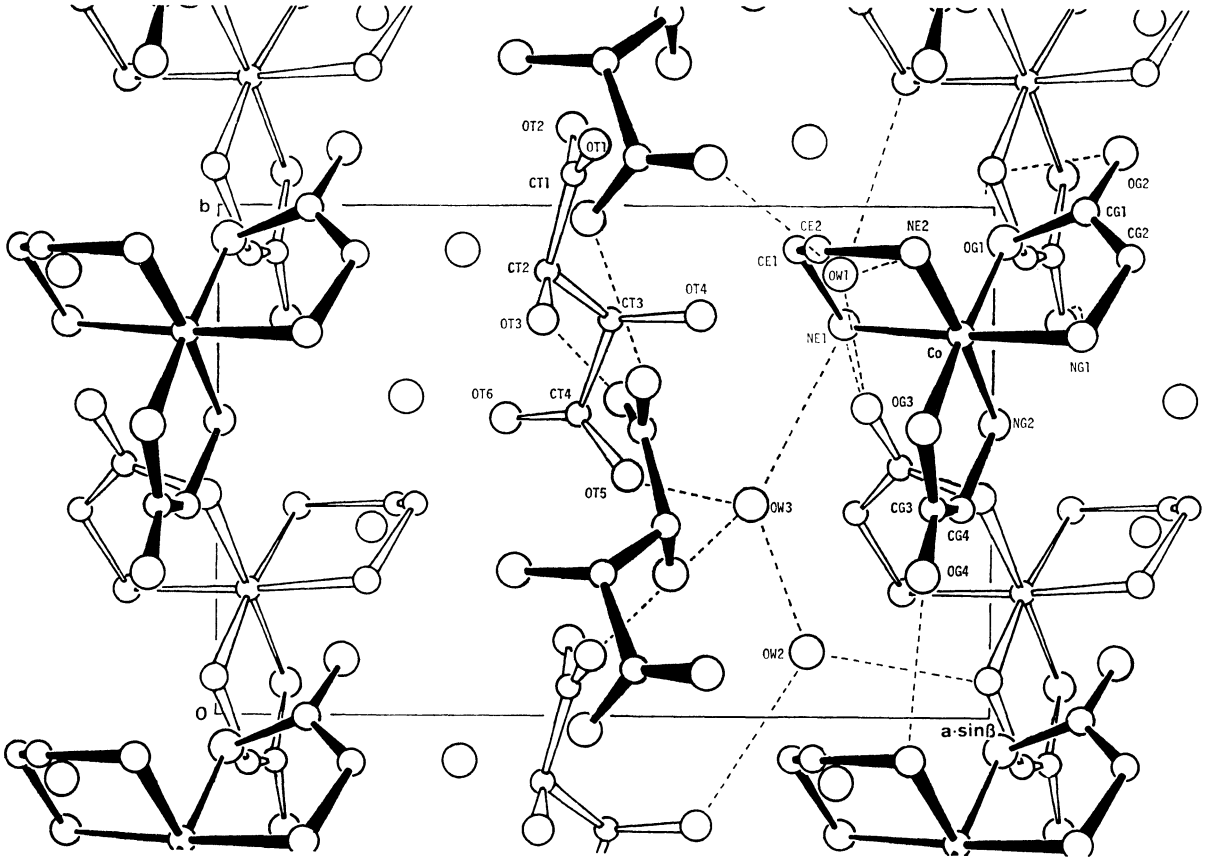

Fig. 1. Projection of the crystal structure along the c-axis of the less-soluble salt, $(+)_{589}$-*trans*(*O*)-[Co(gly)$_2$en]H-*d*-tart·$3H_2O$. Possible hydrogen bonds are indicated by broken lines.

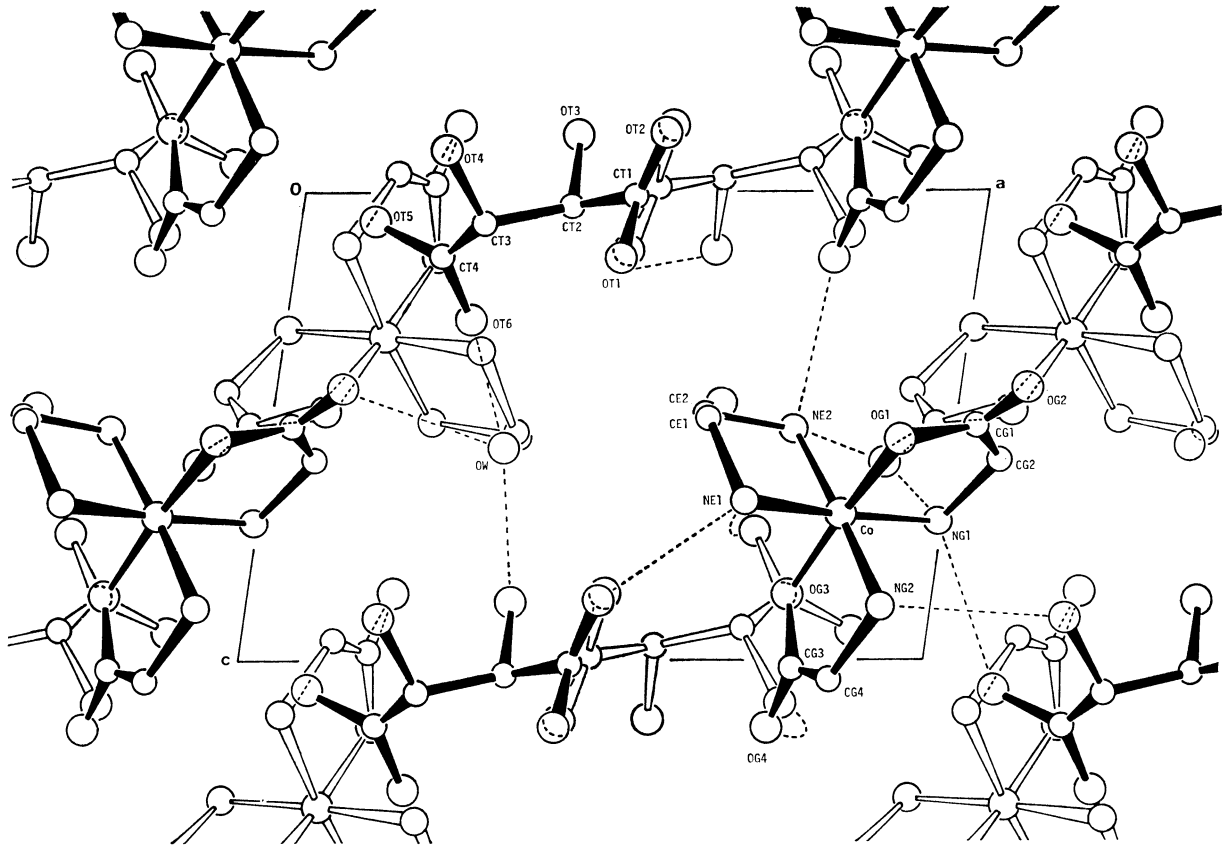

Fig. 2. Projection of the crystal structure along the b-axis of the more-soluble salt, $(-)_{589}$-*trans*(*O*)-[Co(gly)$_2$en]H-*d*-tart·H$_2$O. Possible hydrogen bonds are indicated by broken lines.

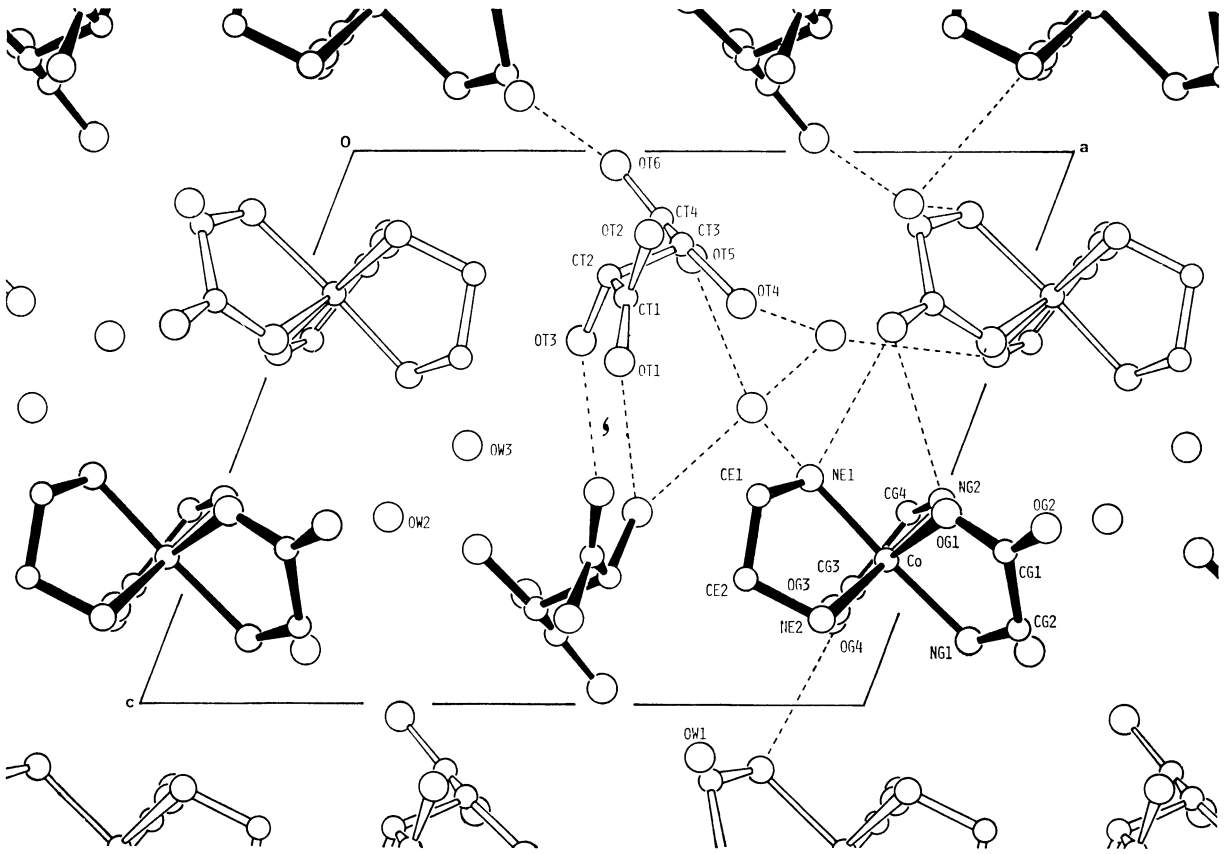

Fig. 3. Projection of the crystal structure along the b-axis of the less-soluble salt, $(+)_{589}$-*trans*(*O*)-[Co(gly)$_2$en]H-*d*-tart·3H$_2$O. Possible hydrogen bonds are indicated by broken lines.

factors (B=4.0 Å^2) converged to R=0.043 (the refinement of the inverted structure gave R=0.045). A final difference map showed no peaks higher than 0.5 electron/Å^3. The quantity minimized was $w(|F_o|-k|F_c|)^2$. Cruickshank's weighting scheme[4] was used, where $w=1/(a+|F_o|+b|F_o|^2)$, with a=6.50 and b=0.019. The atomic scattering factors from the International Tables for X-Ray Crystallography[5] were used. The effect of the anomalous dispersion of the Co atom was included in the calculation: the values of $\Delta f'$=0.299 and $\Delta f''$=0.973 for Mo $K\alpha$ radiation were also taken from the International Tables for X-Ray Crystallography.[6]

The More-soluble Salt, (−)$_{589}$-trans(O)-[Co(gly)$_2$en]-H-d-tart·H$_2$O (2). The determination and the refinement of the structure were made in a way similar to those used for **1**. The final refinement converged to R=0.064 (the inverted structure gave R=0.067). A final difference map revealed no peaks higher than 0.4 electron/Å^3. A weighting scheme similar to that used in the case of **1** was used, with a=15.00 and b=0.016.

All the computations were carried out by a HITAC-8700 computer at the Hiroshima University Computer Center. The computer programs used were FOUR-2/M (Fourier synthesis)[7] and HBLS-IV (Least-square calculation), with a slight modification.[8] The final atomic parameters and temperature factors (with their estimated standard deviations) for both salts are listed in Tables 2—5. For both salts, complete lists of the 10$|F_o|$ and 10$|F_c|$ values have been preserved by the Chemical Society of Japan (Document No. 7937).

Results and Discussion

Geometry and Absolute Configuration of Cations. The bond distances and angles within the complex cation of the less- and more-soluble salts are listed in Tables 6 and 7. All the distances and angles are in good agreement with the reported values.[1,2,9-12]

The absolute configuration of the (+)$_{589}$-*trans*(*O*)-[Co(gly)$_2$en]$^+$ cation was identified as *Λ*-*δ*[13] on the basis of that of the hydrogen-*d*-tartrate used as an internal reference.[14,15] Similarly, that of the (−)$_{589}$-*trans*(*O*)-[Co(gly)$_2$en]$^+$ cation was identified as *Δ*-*λ*. These assignments are in accordance with those proposed

Table 8. Intermolecular distances (≤3.28 Å) for (+)$_{589}$-*trans*(*O*)-[Co(gly)$_2$en]H-*d*-tart·3H$_2$O

D–H···A[a]	D···A(*l*/Å)	H···A (*l*/Å)	D–H···A (*φ*/°)
N(E1)–H(NE11)···O(W3)^{i}	3.173(8)[b]	2.29	150
N(E1)–H(NE12)···O(T4)	3.235(7)	2.69	114
N(E1)–H(NE12)···O(G2)^{ii}	3.171(7)[b]	2.41	132
N(E2)–H(NE21)···O(G4)^{iii}	2.833(7)[b]	1.91	150
N(E2)–H(NE22)···O(W1)	3.128(7)[b]	2.38	130
N(G1)–H(NG11)···O(W1)^{v}	3.094(8)[b]	2.19	153
N(G1)–H(NG12)···O(G4)^{vi}	2.896(8)[b]	1.88	178
N(G2)–H(NG21)···O(W2)^{vii}	2.875(10)[b]	1.90	163
N(G2)–H(NG22)···O(G1)^{ii}	3.033(6)	2.35	124
N(G2)–H(NG22)···O(G2)^{ii}	3.128(6)[b]	2.17	155
O(G2)···O(T4)^{viii}	2.895(6)	—	—
O(W1)^{vi}–H(OW1)···O(G2)	2.955(7)[b]	2.30	154
O(G2)···O(W3)^{vii}	3.161(8)	—	—
C(E2)···O(W1)	3.117(10)	—	—
C(G3)···O(W1)^{v}	3.110(8)	—	—
C(G4)–H(CG42)···O(W3)^{i}	3.244(9)	2.33	145
C(G4)···O(W1)^{v}	3.148(8)	—	—
O(G4)···C(E2)^{ix}	3.207(10)	—	—
N(G1)–H(NG11)···O(T6)^{iv}	3.274(7)	2.58	128
O(T1)···O(W3)^{x}	3.258(10)	—	—
O(T3)^{x}–H(OT3)···O(T1)	2.906(9)[b]	2.30	124
O(T2)–H(OT2)···O(T5)^{iii}	2.608(7)[b]	1.80	173
O(W3)–H(OW32)···O(T3)	2.843(8)[b]	2.03	171
O(W2)^{x}–H(OW21)···O(T4)	3.017(10)[b]	2.40	130
O(W3)^{x}–H(OW31)···O(T5)	2.806(8)[b]	2.09	145
O(W1)–H(OW12)···O(T6)^{x}	2.650(7)[b]	2.02	124
O(W2)–H(OW22)···O(W3)	2.919(11)[b]	2.07	159

Roman numerals as superscripts refer to the following equivalent positions relative to the reference molecule at x, y, z:

i(1−x, −1/2+y, 1−z),	ii(2−x, −1/2+y, 1−z)
iii(x, 1+y, z),	iv(1+x, y, 1+z)
v(2−x, −1/2+y, 2−z),	vi(2−x, 1/2+y, 2−z)
vii(1+x, y, z),	$viii$(2−x, 1/2+y, 1−z)
ix(x, −1+y, z),	x(1−x, 1/2+y, 1−z)

a) D, hydrogen donor; A, hydrogen acceptor. b) Possible hydrogen bonds.

by Dabrowiak and Cooke[3] based on the CD spectral pattern. The projections of the crystal structure of **1** along the c-axis and that of **2** along the b-axis are shown in Figs. 1 and 2 respectively. These projections correspond to the figure viewed along the guasi-threefold axis of each complex cation.

Anion Geometry. The bond distances and angles of the H-*d*-tart anions in both crystals are in accordance

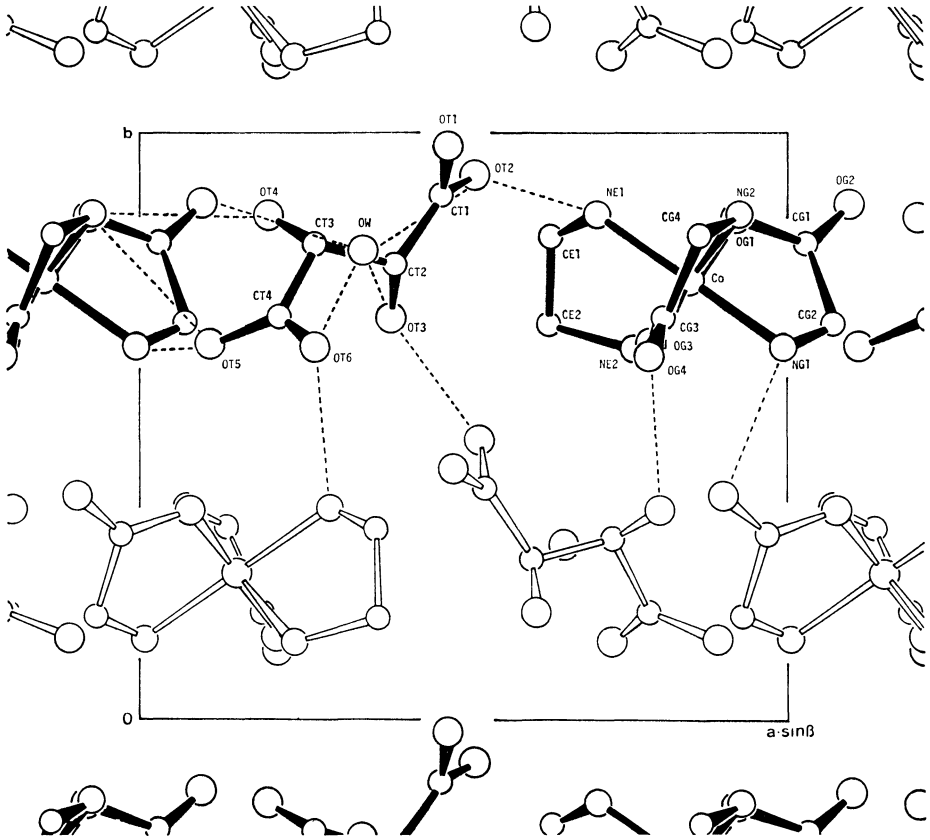

Fig. 4. Projection of the crystal structure along the c-axis of the more-soluble salt, $(-)_{589}$-*trans*(*O*)-[Co(gly)$_2$en]H-*d*-tart·H$_2$O. Possible hydrogen bonds are indicated by broken lines.

Table 9. Intermolecular distance ($\leq$3.28 Å) for $(-)_{589}$-*trans*(*O*)-[Co(gly)$_2$en]H-*d*-tart·H$_2$O

D–H···A[a]	D···A (l/Å)	H···A (l/Å)	D–H···A (ϕ/°)
N(E1)^{i}–H(NE11)···O(T6)	2.785(10)[b]	1.82	155
N(E1)–H(NE12)···O(T2)^{ii}	2.962(14)[b]	2.08	148
N(E2)–H(NE21)···O(G2)^{iii}	2.978(10)[b]	2.16	140
N(E2)–H(NE22)···O(G4)^{viii}	2.867(11)[b]	1.95	150
N(G1)–H(NG11)···O(G2)^{iii}	2.907(10)[b]	1.96	161
N(G1)–H(NG12)···O(T5)^{v}	2.833(10)[b]	1.84	168
N(G2)–H(NG22)···O(T4)^{v}	2.978(10)[b]	2.00	164
N(G2)–H(NG22)···O(T5)^{v}	3.152(10)	2.50	122
OW^{vi}–H(OW2)···O(G2)	2.929(12)[b]	2.16	132
O(T4)^{i}–H(OT4)···O(G4)	2.715(11)[b]	1.86	149
OW–H(OW1)···O(T6)	2.713(12)[b]	1.91	174
OW···O(T2)^{ii}	3.161(15)	—	—
O(T3)^{ii}–H(OT3)···OW	2.731(12)[b]	1.90	155
O(T1)^{vii}–H(OT1)···O(T3)	2.579(11)[b]	1.68	145

Roman numerals as superscripts refer to the following equivalent positions relative to the reference molecule at x, y, z:

i $(1-x, -1/2+y, 1-z)$,	ii $(x, y, 1+z)$
iii $(2-x, -1/2+y, 1-z)$,	iv $(-1+x, y, -1+z)$
v $(1+x, y, 1+z)$,	vi $(1+x, y, z)$
vii$(1-x, -1/2+y, -z)$,	viii $(x, y, -1+z)$

a) D, hydrogen donor; A, hydrogen acceptor. b) Possible hydrogen bonds.

with the previously reported values.[1,2,16] The five nonhydrogen atoms of each α-hydroxycarboxylate moiety lie approximately on a plane. The angle between the planes of the two α-hydroxycarboxylate moieties in the less-soluble salt (**1**) is nearly equal to the corresponding angle of the H-*d*-tart anion in **3** (55.4° *vs.* 55.8°[1]). On the other hand, the corresponding value in the more-soluble salt (**2**) is 60.9° (61.3° for **4**[2]).

Crystal Packing. *(a) The Less-soluble Salt (**1**)*: The crystal structure consists of discrete $(+)_{589}$-*trans*(*O*)-$[Co(gly)_2en]^+$ cations, H-*d*-tart anions, and water molecules. Figures 1 and 3 show the projections of the crystal structure along the c- and b-axes respectively. The intermolecular distances and angles are summarized in Table 8.

In the crystal there are two distinct layers, as is shown in Figs. 1 and 3. The first layer is formed by H-*d*-tart anions. The H-*d*-tart anions are arranged to form a double-chain structure along the twofold screw axis at ($x=1/2$, $z=1/2$). Here, each component chain itself has a "head-to-tail" arrangement formed by a unit translation of the H-*d*-tart anion along the b-axis. The O(T2)···O(T5)^{iii} distance, 2.608 Å, is slightly longer than those in **3** and **4** (2.44 and 2.47 Å respectively).[1,2] The two-component chains, moreover, are linked to each other through the hydrogen bonds (O(T1)···O(T3)^{x} 2.906 Å) and are related by the twofold screw axis. These double-chain structures, then, are related to each other by the twofold screw axis at ($x=1/2$, $z=0$) to form the layer parallel to the bc plane.

The second layer is built up of the complex cations. The layer of the complex cation is constructed by the same symmetry operation as in the case of the H-*d*-tart anion, as is shown in Figs. 1 and 3.

The first and second layers are not only directly adjoined with each other by short contacts: N(E1)··· O(T4) 3.235, O(G2)^{ii}···O(T4) 2.895, and N(G1)··· O(T6)^{iv} 3.274 Å, but are also indirectly joined together by hydrogen bonds *via* the waters of crystallization: O(T6)···O(W1)···O(G2), O(T6)···O(W1)···N(E2), O(T6)···O(W1)···N(G1), O(T4)···O(W2)···N(G2), O(T3)···O(W3)···N(E1), and O(T5)···O(W3)···N(E1).

*(b) The More-soluble Salt (**2**)*: Figures 2 and 4 show the projections of the crystal structure of **2** along the b- and

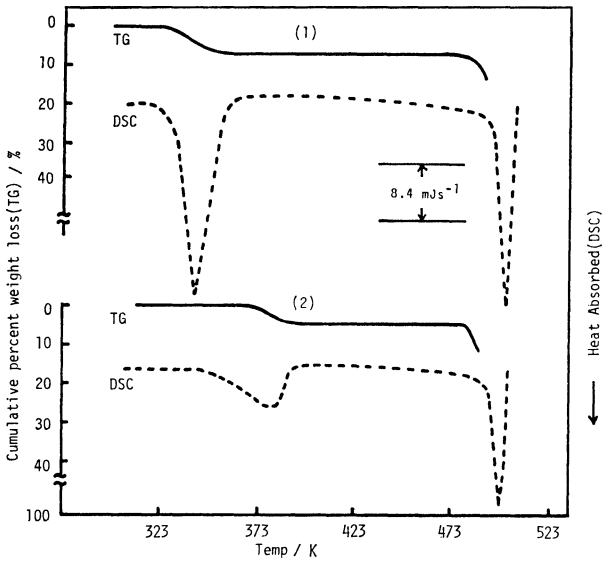

Fig. 5. TG and DSC curves of both diastereoisomers: (1) the less-soluble salt, $(+)_{589}$-*trans*(*O*)-$[Co(gly)_2en]$-H-*d*-tart·$3H_2O$; (2) the more-soluble salt, $(-)_{589}$-*trans*-(*O*)-$[Co(gly)_2en]$H-*d*-tart·H_2O.

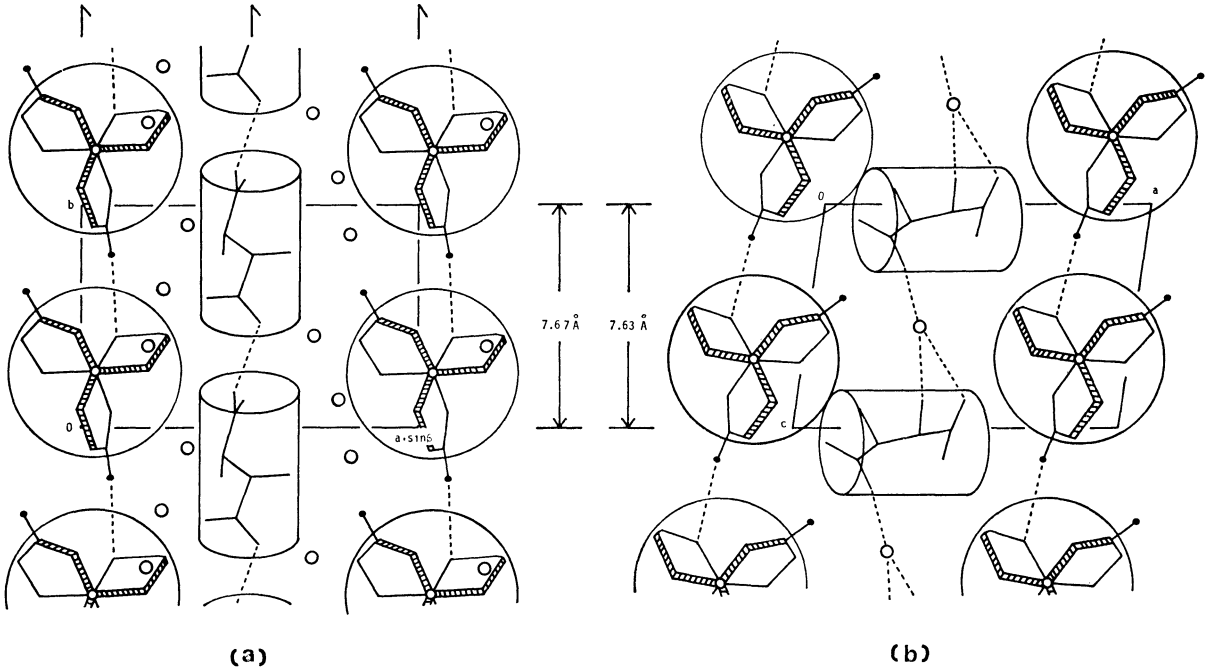

Fig. 6. A schematic drawing of the bounded projections of the less- and more-soluble diastereoisomers: (a) $(+)_{589}$-*trans*(*O*)-$[Co(gly)_2en]$H-*d*-tart·$3H_2O$(c-axis projection), (b) $(-)_{589}$-*trans*(*O*)-$[Co(gly)_2en]$-H-*d*-tart·H_2O(b-axis projection).
Broken lines denote hydrogen bonds and small circles indicate water molecules.

c-axes respectively. The structure consists of the discrete $(-)_{589}$-*trans*(*O*)-[Co(gly)$_2$en]$^+$ cations, the H-*d*-tart anions, and the water molecules. The intermolecular distances and angles are listed in Table 9. In the crystal, the complex cations are stacked to form a chain by hydrogen bonds along the c-axis. The hydrogen bond distance, N(E2)···O(G4)^{viii}, is 2.867 Å. Along the c-axis, the H-*d*-tart anions do not form the "head-to-tail" chain structure, though they are connected to each other through the water of crystallization.

Thermal Behavior of the Water of Crystallization. The results of the TG and DSC measurements of both diastereoisomers are shown in Fig. 5. The crystals of the less-soluble salt (**1**) begin to release the water of crystallization at 327 K, and the dehydration ceases at 347 K. The weight loss accompanying this dehydration is found to be 9.7%. This value is very close to the value expected for the dehydration of 2.5H$_2$O (9.6%). The DSC peak is observed from 329 K to 354 K. The ΔH value for the dehydration is calculated to be 64.4 kJ mol^{-1}.

On the other hand, the more-soluble salt (**2**) loses 0.7 mol of the water of crystallization in the temperature range between 368 K and 382 K (TG curve). The DSC peak corresponding to this step is observed from 347 K to 389 K. The ΔH value for the dehydration step is found to be 73.0 kJ mol^{-1}, slightly larger than that of the less-soluble salt. The gradual decrease in both DSC curves in the range of about 420—470 K is probably due to the loss of the remaining water of crystallization (0.5H$_2$O for **1** and 0.3H$_2$O for **2**). The DSC peak was also found at about 500 K in both samples. While the TG measurement was being carried out, the samples got black and swelled above 490 K. The measurements was impossible above this temperature. It seems that the decomposition of both samples occurs at 490 K.

Thus, the less-soluble salt (**1**) (containing more water, trihydrate) has been proved to release water more easily than the more-soluble salt (**2**) (containing less water, monohydrate).

Comparison of the Packing Modes of the Less- and More-soluble Salts. The two crystal structures are shown schematically in Fig. 6, where the H-*d*-tart anions are depicted in a cylindrical form and the complex cations are represented as a large circle. There are some resemblances and differences between the packing modes of the two structures. The resemblances are: (1) The complex cations are stacked along the longitudinal axis in the figure, making a chain structure by the N–H···O hydrogen bonds in both crystals. (2) Unit translation along both longitudinal axes are quite similar; the distances are 7.67 Å for **1** and 7.63 (c×sinβ) for **2**. The differences are: (1) In Fig. 6(a), the H-*d*-tart anions are linked with hydrogen bonds (–COOH···OOC–) just as the dry cells are arranged in a series circuit. In contrast, the H-*d*-tart anions in Fig. 6(b) are connected to each other *via* water molecules, COO···water $\cdots\begin{Bmatrix}\text{OH}\\\text{COO}\end{Bmatrix}$, just as the dry cells are piled side by side in a parallel form. (2) A layer of water molecules exists in Fig. 6(a), but not in Fig. 6(b).

The crystal parameters of the two diastereoisomeric pairs are listed in Table 1. Since **2** and **3** have the same chemical formula, $C_{10}H_{23}N_4O_{11}Co$, the V/Z value of **2** should be nearly equal to that of **3**. However, the volume of **3** is 18.2 Å^3 smaller than that of **2**. The volume difference between **1** and **3** is 43.3 Å^3. This difference is nearly equal to twice the reported molecular volume of the water of crystallization (2×20.6 Å^3),[17] and can be attributed to the two excess water molecules in **1**. Hence, **1** is as dense as **3**. Consequently, in spite of the presence of more water of crystallization, the less-soluble salt (**1**) is more tightly packed than the more-soluble salt (**2**).

The situation is quite similar to the case in the diastereoisomeric pair of **3** and **4**. The volume difference between **3** and **4** is 27.2 Å^3. Since **4** has one more water molecule than **3**, this volume difference corresponds to the volume of one water molecule in **4**. The observed volume difference (27.2 Å^3) is 6.6 Å^3 larger than the expected volume for one water molecule.[17] Therefore, it may be inferred that **3** is more tightly packed than **4**.

The crystal structures of the less-soluble salts, **1** and **3**, contain the spiral chain of H-*d*-tart. In contrast, the more-soluble salts, **2** and **4**, do not have such spiral chains. Therefore, it can be considered that the tight packing in the less-soluble salt is caused by the existence of this spiral chain of H-*d*-tart. In other words, the existence of this spiral chain of H-*d*-tart plays a decisive role in the discrimination between Δ and Λ enantiomers. This conclusion is supported by the fact that several less-soluble salts of organic bases, (—)-adrenalinium H-*d*-tart,[16] (+)-[(—)-1-methyl-3-benzoylpiperidinium H-*d*-tart]H$_2$O,[18] and (—)-[(—)-1-methyl-3-ethyl-3-benzoylpiperidinium H-*d*-tart],[19] contain similar spiral chains of the H-*d*-tart anion in the crystal structures.

Additionally, a pitch of the spiral chain is considered important in the discrimination due to the H-*d*-tart anion. The observed length of the chain pitch (7.1—7.8 Å)* is nearly equal to the diameter of the complex cations, [Co(ox)en$_2$]$^+$ and [Co(gly)$_2$en]$^+$. These complex cations can themselves form a chain by hydrogen bonds (N–H···O) within the range of this pitch (7.1—7.8 Å). Other complex cations so far resolved by the H-*d*-tart anion are as follows: *β-cis*(*O*)-[Co(gly)$_2$en]$^+$,[3] *s-cis*-[Co(edda)(NH$_3$)$_2$]$^+$,[20] *trans*-[Co(edda)en]$^+$,[21] and *s-cis*-[Co(dmedda)(NH$_3$)$_2$]$^+$.[20],** The sizes and the skeletons of these complexes have a close resemblance to those of the [Co(ox)en$_2$]$^+$ and *trans*(*O*)-[Co(gly)$_2$en]$^+$ cations, as is shown in Fig. 7. The figure shows that the monovalent complex cation satisfying the following conditions has a great chance of optical resolution by way of the diastereoisomeric salt formation with the H-*d*-tart anion: (1) the complex cation has carboxyl and amino groups at the *trans* or *cis* positions of octahedral coordination, so that cations

* The chain pitches of the H-*d*-tart anion have values within 7.1—7.8 Å in Refs. 1, 2, 16, 18, and 19.

** The abbreviations used for the ligands are as follows: gly, glycinate anion; en, ethylenediamine; edda, ethylenediamine-*N*,*N*′-diacetate anion; dmedda, dimethylethylenediamine-*N*,*N*′-diacetate anion.

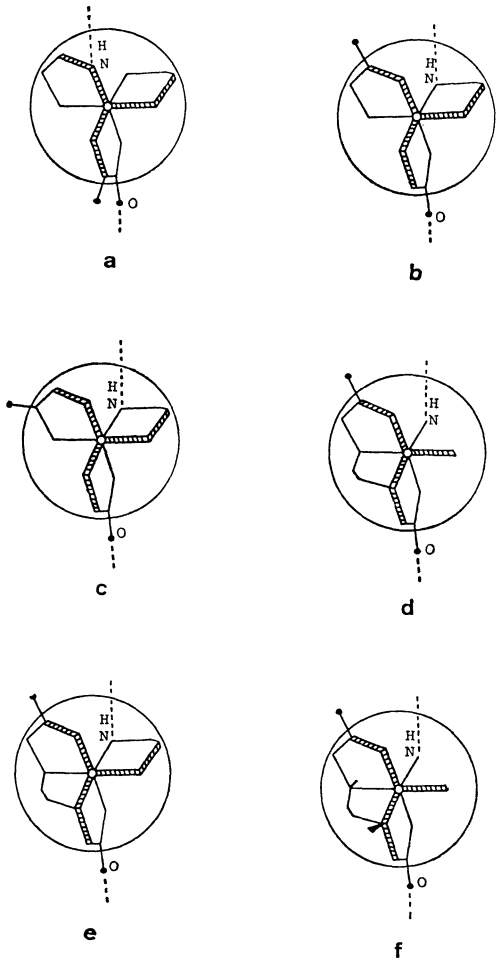

Fig. 7. A schematic drawing of monovalent complex cations having a structural resemblance to $(+)_{589}$-[Co(ox)en_2]$^+$ and $(+)_{589}$-*trans*(*O*)-[Co(gly)$_2$en]$^+$: (a) $(+)_{589}$-[Co(ox)en_2]$^+$, (b) $(+)_{589}$-*trans*(*O*)-[Co(gly)$_2$en]$^+$, (c) *β-cis*(*O*)-[Co(gly)$_2$en]$^+$, (d) *s-cis*-[Co(edda)$(NH_3)_2$]$^+$, (e) *trans*-[Co(edda)en]$^+$, and (f) *s-cis*-[Co(dmedda)$(NH_3)_2$]$^+$.

can be linked with each other by N–H···O type hydrogen bonds, and (2) the complex cation is 7.1—7.8 Å in diameter, so that the complex cations can be arranged in a spiral chain with the same pitch as that of the H-*d*-tart spiral chain.

The author wishes to express his thanks to Professor Hayami Yoneda and Dr. Yoshihiko Kushi of Hiroshima University for their kind guidance and encouragement throughout this work, and also to Dr. Ushio Sakaguchi and to Dr. Katsuhiko Miyoshi for their stimulating discussion and helpful suggestions. The author is also grateful to Dr. Kozo Akabori, Hiroshima University, for the TG and DSC measurements and for his valuable suggestions; thanks are also due to the Hiroshima University Computer Center for a generous allocation of computer time.

References

1) M. Kuramoto, Y. Kushi, and H. Yoneda, *Bull. Chem. Soc. Jpn.*, **51**, 3251 (1978).
2) M. Kuramoto, Y. Kushi, and H. Yoneda, *Bull. Chem. Soc. Jpn.*, in press.
3) J. C. Dabrowiak and D. W. Cooke, *Inorg. Chem.*, **14**, 1305 (1975).
4) D. W. J. Cruickshank, "Computing Methods and the Phase Problem in X-ray Crystal Analysis," ed by R. Pepinsky, J. M. Robertson, and J. C. Speakman, Pergamon Press, Oxford (1961), p. 45.
5) "International Tables for X-Ray Crystallography," Kynoch Press, Birmingham (1968), Vol. III, pp. 201—206.
6) "International Tables for X-Ray Crystallography," Kynoch Press, Birmingham (1974), Vol. IV, p. 148.
7) Y. Kushi, unpublished work.
8) T. Ashida, "The Universal Crystallographic Computation Program System," ed by T. Sakurai, The Crystallographic Society of Japan (1967).
9) H. Miyamae and Y. Saito, *Acta Crystallogr., Sect. B*, **34**, 937 (1978).
10) P. Vasić, R. Herak, and S. Djurić, *Acta Crystallogr., Sect. B*, **32**, 91 (1976).
11) L. J. Halloran, R. C. Caputo, R. D. Willett, and J. I. Legg, *Inorg. Chem.*, **14**, 1762 (1975).
12) Y. Mitsui, J. Watanabe, Y. Harada, T. Sakamaki Y. Iitaka, Y. Kushi, and E. Kimura, *J. Chem. Soc., Dalton, Trans.*, **1976**, 2095.
13) IUPAC, *Inorg. Chem.*, **9**, 1 (1970).
14) A. J. van Bommel and J. M. Bijvoet, *Acta Crystallogr.*, **11**, 61 (1958).
15) The application of Hamilton's *R*-factor ratio test (*Acta Crystallogr.*, **18**, 502 (1965)) gave 0.045/0.043=1.05 for **1** and 0.067/0.064=1.05 for **2**. Therefore, the hypothesis that the inverted structure is correct can be rejected at the 0.5% significance level.
16) D. Carlström, *Acta Crystallogr., Sect. B*, **29**, 161 (1973).
17) K. Harata, *Bull. Chem. Soc. Jpn.*, **49**, 2066 (1976).
18) G. Hite and J. R. Soares, *Acta Crystallogr., Sect. B*, **29**, 2935 (1973).
19) J. R. Ruble, G. Hite, and J. R. Soares, *Acta Crystallogr., Sect. B*, **32**, 136 (1976).
20) W. T. Jordan and B. E. Douglas, *Inorg. Chem.*, **12**. 403 (1973).
21) J. I. Legg, D. W. Cooke, and B. E. Douglas, *Inorg, Chem.*, **6**, 700 (1967).